Cancer Chemother Pharmacol (2006) 58: 725–734
DOI 10.1007/s00280-006-0207-8

ORIGINAL ARTICLE

**Theodore J. Lampidis · Metin Kurtoglu
Johnathan C. Maher · Huaping Liu · Awtar Krishan
Valerie Sheft · Slawomir Szymanski · Izabela Fokt
Witold R. Rudnicki · Krzysztof Ginalski
Bogdan Lesyng · Waldemar Priebe**

Efficacy of 2-halogen substituted D-glucose analogs in blocking glycolysis and killing "hypoxic tumor cells"

Received: 11 October 2005 / Accepted: 1 February 2006 / Published online: 23 March 2006

Abstract *Purpose*: Since 2-deoxy-D-glucose (2-DG) is currently in phase I clinical trials to selectively target slow-growing hypoxic tumor cells, 2-halogenated D-glucose analogs were synthesized for improved activity. Given the fact that 2-DG competes with D-glucose for binding to hexokinase, in silico modeling of molecular interactions between hexokinase I and these new analogs was used to determine whether binding energies correlate with biological effects, i.e. inhibition of glycolysis and subsequent toxicity in hypoxic tumor cells. *Methods and Results*: Using a QSAR-like approach along with a flexible docking strategy, it was determined that the binding affinities of the analogs to hexokinase I decrease as a function of increasing halogen size as follows: 2-fluoro-2-deoxy-D-glucose (2-FG) > 2-chloro-2-deoxy-D-glucose (2-CG) > 2-bromo-2-deoxy-D-glucose (2-BG). Furthermore, D-glucose was found to have the highest affinity followed by 2-FG and 2-DG, respectively. Similarly, flow cytometry and trypan blue exclusion assays showed that the efficacy of the halogenated analogs in preferentially inhibiting growth and killing hypoxic vs. aerobic cells increases as a function of their relative binding affinities. These results correlate with the inhibition of glycolysis as measured by lactate inhibition, i.e. ID50 1 mM for 2-FG, 6 mM for 2-CG and > 6 mM for 2-BG. Moreover, 2-FG was found to be more potent than 2-DG for both glycolytic inhibition and cytotoxicity. *Conclusions*: Overall, our in vitro results suggest that 2-FG is more potent than 2-DG in killing hypoxic tumor cells, and therefore may be more clinically effective when combined with standard chemotherapeutic protocols.

Keywords 2-Deoxy-D-glucose · 2-Fluoro-2-deoxy-D-glucose · Hypoxia · Glycolysis · Antitumor activity

T. J. Lampidis · M. Kurtoglu · J. C. Maher · H. Liu
A. Krishan · V. Sheft
School of Medicine and Sylvester Cancer Center,
The University of Miami, Miami, FL, USA

S. Szymanski · I. Fokt · W. Priebe (✉)
Department of Experimental Therapeutics,
The University of Texas M. D. Anderson Cancer Center,
1515 Holcombe Blvd., Houston, TX 77030, USA
E-mail: wp@wt.net
Tel.: +1-713-7923777
Fax: +1-713-7454975

W. R. Rudnicki · K. Ginalski · B. Lesyng
Interdisciplinary Center for Mathematical and Computational Modeling, Warsaw University, Warsaw, Poland

B. Lesyng
Department of Biophysics, Warsaw University, Warsaw, Poland

Introduction

The use of 2-deoxy-2-fluoro-D-glucose (2-FG) to localize human tumors in patients by PET scan has been a valuable tool in determining the extent of disease as well as the outcome of therapy [9, 10, 17, 32, 37, 40]. In a series of recent papers, we have shown that the related analog, 2-deoxy-D-glucose (2-DG), as well as other inhibitors of glycolysis, preferentially inhibit growth, and kill human osteosarcoma cells grown under three different conditions of simulated hypoxia as compared with the same cells growing under normal oxygen tension [18, 20, 21].

The basis for the in vivo tumor localization of 2-FG as well as preferential killing of cells under hypoxia by 2-DG derives from a number of factors, which include, but are not limited to, (a) upregulation of glucose transporters in tumor cells [12, 27, 33], (b) competition with glucose for transporters as well as hexokinases [38], (c) preferential accumulation in tumor versus normal cells of 2-deoxy-6-phosphate-D-glucose (2-DG-6P) or 2-FG-6P, due to over expression of kinases and reduced expression of phosphatases [42], (d) the inability of the phosphorylated analogs to be converted to fructose-6-phosphate by the isomerase, and thus competitively blocking this step of glycolysis [5, 25, 26, 37, 41], and (e)

the incapacity of tumor cell mitochondria in an hypoxic microenvironment to process other sources of energy (such as fats and proteins) for ATP production.

We recently demonstrated that 2-DG can be used in conjunction with standard chemotherapeutic agents to raise the efficacy of these treatments in human xenograft models in vivo [16, 24]. The rationale for this combinative treatment is based on the understanding that traditional chemotherapeutic agents are limited in that they target rapidly dividing cells (whether tumor or normal) while the slow-growing cells of a tumor remain relatively resistant. However, these slow-growing tumor cell populations can be selectively distinguished from slow-growing normal cells due to their hypoxic microenvironment. Thus, inhibitors of glycolysis, such as 2-DG, should have increased cytostatic as well as cytotoxic effects on these oxygen-deprived tumor cells as compared to the rest of the normally oxygenated slow-growing cells in the body [18, 20, 21]. On the basis of this rationale, phase I clinical trials have recently begun at the University of Miami Sylvester Cancer Center using 2-DG to target the slow-growing hypoxic cells in combination with docetaxel, which attacks the rapidly dividing aerobic cells (protocol no. 2003121, "a phase I dose escalation trial of 2-DG alone and in combination with docetaxel in subjects with advanced solid malignancies").

Comparing 2-FG to 2-DG, the fluorine in 2-FG can be considered to be similar in size to hydrogen at this position in 2-DG. However, fluorine's electronic effects more closely resemble those of the hydroxyl group at the C-2 position of glucose then the H at the same position in 2-DG. These considerations prompted us to determine whether 2-FG would be more effective than 2-DG in shutting down glycolysis and killing hypoxic cells. Using molecular modeling, glycolysis inhibition assays, growth inhibitory assays, and death assays, we assessed the effects of 2-FG, as well as other synthesized halogen-substituted glucose analogs, i.e. 2-chloro-2-deoxy-D-glucose (2-CG) and 2-bromo-2-deoxy-D-glucose (2-BG), and compared them with those of 2-DG in a genetic and environmental tumor cell model of hypoxia."

Materials and methods

Cell types

An osteosarcoma cell line 143B (wt.) was exposed to ethidium bromide for prolonged periods, and a mutant cell line with complete loss of mtDNA (ρ^o) was selected [14]. Since, the ρ^o cells are uridine and pyruvate auxotrophs, they were grown in DMEM supplemented with 10% fetal calf serum, 50 μg/ml uridine, 100 mM sodium pyruvate, 4.5 mg/ml glucose, and 10 μg/ml gentamycin. To maintain standard experimental conditions, the parental cell line (wt.) was grown in the same medium. Due to absence of mtDNA, ρ^o cells are unable to perform oxidative phosphorylation. Thus, throughout the paper we refer to ρ^o cells as our genetic model of "hypoxia," even though all experiments were performed under normoxic conditions, while the wt parental 143B cells were used as the aerobic control. This model of simulated hypoxia was selected since it does not express hypoxia inducible factor (HIF), and therefore can be compared to our environmental model, which does as described below.

Environmental model of hypoxia

For studies on glycolytic inhibitors in the environmental model of hypoxia, cells were seeded and incubated for 24 h at 37°C in an atmosphere containing 5% CO_2 as described below (growth inhibition and direct cytotoxicity assays). After 24 h incubation, cells received drug treatment and were placed in a Pro-Ox in vitro chamber attached to a model 110 oxygen controller (Reming Bioinstruments, Redfield, NY). A mixture of 95% nitrogen and 5% CO_2 was used to perfuse the chamber to achieve the desired oxygen level (0.5%). Hypoxic treatment was continuous for 72 h.

Drugs

2-DG was purchased from Sigma, St. Louis, Missouri. The 2-FG, 2-CG, and 2-BG were synthesized according to existing procedures [1, 2, 7, 28, 39], and their structures were confirmed by ^{1}H and ^{13}C NMR spectrometry. Figure 1 illustrates the structure of each molecule.

Analytical data for synthesized alpha and beta anomeric mixtures of 2-halo-D-glucose derivatives

2-Deoxy-2-fluoro-α,β-D-glucose (2-FG)

^{1}H NMR (D_2O, δ): 5.33 (d, $J = 3.8$ Hz, H-1α), 4.79 (dd, $J = 7.8$, 2.2 Hz, H-1β), 4.30 (ddd, $J = 49.41$, 9.5, 3.9 Hz, H-2α), 3.98 (ddd, $J = 51.4$, 8.8 Hz, H-2β), 3.86 (ddd, $J = 18.8$, 13.3, 9.4 Hz, H-3α), 3.85–3.65 (m, H-6α,β, 3β, 5β), 3.42–3.33 (m, H-4α,β, H-5α).

^{13}C NMR (D_2O, δ): 93.5 (d, $J = 13.9$ Hz, C-1β), 92.79 (d, $J = 94.5$ Hz, C-2β), 92.26 (d, $J = 105.8$ Hz, C-2α), 89.62 (d, $J = 18$ Hz, C-1α), 76.02 (C-5α), 74.03 (d, $J = 10.3$ Hz, C-3β), 71.25 (C-5β), 71.15 (d, $J = 13.5$ Hz, C-3α), 69.28 (d, $J = 4.9$ Hz, C-4β), 69.13 (d, $J = 4.8$ Hz, C-4α).

FAB-MS: m/e 181.2

2-Chloro-2-deoxy-α,β-D-glucose (2-CG)

^{1}H NMR (D_2O, δ): 5.25 (d, $J = 3.1$ Hz, H-1α), 4.74 (d, $J = 8.2$ Hz, H-1β), 3.89–3.76 (m, H-2α, 5α, 6α, 6β), 3.74 (dd, $J = 10.7$, 5.6 Hz, H-4α), 3.69 (dd, $J = 12.4$, 5.8 Hz, H-3α), 3.60 (dd, $J = 10.1$, 8.8 Hz, H-4β), 3.53 (dd, $J = 10$,

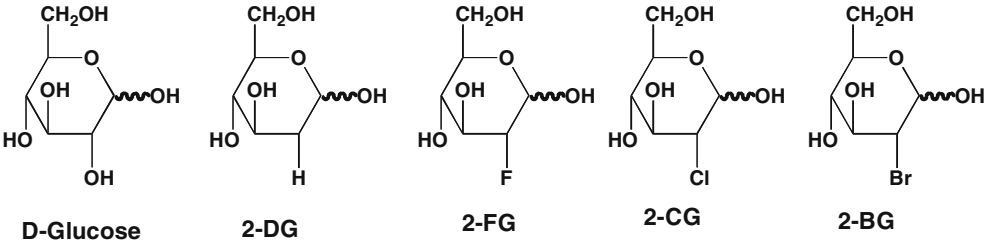

Fig. 1 Structures of D-glucose and its analogs: 2-deoxy- (2-DG), 2-fluoro- (2-FG), 2-chloro- (2-CG), and 2-bromo- D-glucose (2-BG)

8.3 Hz, H-2β), 3.5–3.47 (m, H-5β), 3.43 (dd, $J=10.1$, 8.8 Hz, H-3α), 3.39 (dd, $J=9.7$ Hz, H-3β).

^{13}C NMR (D_2O, δ): 95.86 (C-1β), 92.09 (C-1α), 76.23 (C-4β), 76.03 (C-5β), 72.85 (C-2α), 71.70 (C-5α), 70.42 (C-3α), 70.10 (C-3β), 63.11 (C-2β), 60.63 (C-6), 60.59 (C-4α), 60.48 (C-6); m.p. 135–136°C.

FAB-MS: m/e 197.2

2-Bromo-2-deoxy-α,β-D-glucose (2-BG)

^{1}H NMR (D_2O, δ): 5.33 (d, 1H, $J=3.1$ Hz, H-1α), 4.88 (d, 1H, $J=8.3$ Hz, H-1β), 3.92–3.58 (m, 7H, H-2α, 2β 4α, 4β, 6α, 6β, 5α), 3.49 (ddd, 1H, $J=8$, 5.6, 2.1 Hz, H-5β), 3.41 (dd, 1H, $J=10$, 8.7 Hz, H-3α), 3.37 (dd, 1H, $J=10$, 8.8 Hz, H-3β).

^{13}C NMR (D_2O, δ): 95.87 (C-1β), 92.29 (C-1α), 76.41 (C-5α), 76.02 (C-5β), 72.85 (C-4α), 71.82 (C-4β), 70.82 (C-3α), 70.44 (C-3β), 60.68 (C-6β), 60.54 (C-6α), 55.66 (C-2β), 52.93 (C-2α); m.p. 75–77°C.

FAB-MS: m/e 241.2

Growth inhibition assays

Two milliliters of 143B (wt.) and ρ^o cells were seeded onto 24-well plates at 4×10^4 and 7×10^4 cells/well, respectively, and incubated at 37°C in 5% CO_2 and 95% air for 24 h. At this time, the medium was removed, replaced by fresh DMEM and drug treatments were then applied continuously for 72 h either under normal oxygen tension (wild type and genetic model of "hypoxia") or under 0.5% oxygen (environmental model of hypoxia). Cells were then harvested, and trypan blue exclusion counts were performed using a hemocytometer. Growth inhibition was determined by the cell count ratio of treated to the respective untreated control sample, and the percentage was calculated for each. Each experiment presented was performed at least twice, and each point represents the average of triplicate samples with standard deviations (SD) indicated.

Direct cytotoxicity assays

Two milliliters of 143B and ρ^o cells were seeded onto 24-well plates at 3×10^4 and 5×10^4 cells/well, respectively. Cells were incubated for 24 h at 37°C and 5% CO_2 Drug treatments were then applied continuously for 72 h either under normal oxygen tension (wild type and genetic model of "hypoxia") or under 0.5% oxygen (environmental model of hypoxia). Cells were then harvested and their respective culture media were collected, combined, and centrifuged at 400 *g* for 5 min. Cell pellets were resuspended in 1 ml of fresh culture medium and 0.5 ml of trypan blue (as an indicator of cell death). Trypan blue-positive cells were scored using a hemocytometer, and the percentage of dead cells was calculated. Each experiment presented was performed at least twice, and each point represents the average of triplicate samples with SD indicated.

Rapid DNA content analysis

Cells were cultured, treated, and pelleted as described above for direct cytotoxicity assays. Cell pellets were resuspended in 1.5 ml of propidium iodide/hypotonic citrate staining solution [15]. Stained nuclei were analyzed in a Coulter XL flow cytometer to determine nuclear DNA content and cell cycle position. A minimum of 10,000 cells was analyzed to generate a DNA distribution histogram.

Lactic acid assay

After cells were rinsed twice with PBS, fresh medium was added to the cultures with and without each of the glucose analogs tested, at the indicated concentrations, and the cells were incubated in 5% CO_2 for 24 h. Then, 0.5 ml of medium was removed from each culture and deproteinated by adding 1 ml of perchloric acid at 8% w/v, vortexing for 30 s, then placing this mixture in 4°C for 5 min, and centrifuging at 1,500 *g* for 10 min. The supernate was centrifuged three times more, to yield a final clear supernate. To determine lactic acid, 0.025 ml of this supernate from treated or non-treated cultures was added to a reaction mixture containing 0.1 ml of lactic dehydrogenase (1,000 units/ml), 2 ml of glycine buffer (glycine, 0.6 mol/l, and hydrazine, pH 9.2), and 1.66 mg/ml NAD. Formation of NADH was measured with a Beckman DU 520 UV/VIS spectrophotometer at 340 nm, which directly corresponded to lactic acid levels as determined by a lactate standard curve. Samples were analyzed in triplicate.

3D Models of human hexokinase I interacting with D-glucose, D-glucose-6-phosphate, and their analogs

Assuming that structurally related ligands have similar binding modes, we built 3D models for complexes of the hexokinase I with glucose/glucose-6-phosphate (G-6P) analogs based on the available crystallographic structure of this protein complexed with glucose and G-6P (PDB code: 1cza) [3] using the INSIGHTII program package (Accelrys Inc., San Diego, CA, USA) (Fig. 2). All modeled complexes encompassed only the C-terminal domain of hexokinase I (composed of two duplicated ribonuclease H-like motifs) whose structure remained unaltered, while glucose and G-6P analogs were derived directly from glucose and G-6P molecules bound in the active site region of the protein, respectively.

Optimization of the 3D structure of the complexes

All models were subjected to a series of energy optimizations with the molecular mechanics (MM) DISCOVER module of INSIGHTII, until the norm of the gradient was smaller than 0.1 kcal/mol Å^2. Energy minimizations were performed in a CFF97 force field [11, 23] with a distance-dependent dielectric constant of 4r, using the steepest descent and conjugate gradient methods. Partial charges for all ligand molecules were calculated using the charge equilibration method [29] implemented using CERIUS2 (Accelrys Inc., San Diego, CA, USA). Main-chain atoms of the protein as well as the heavy atoms of glucose and G-6P analogs were restrained with harmonic forces and a force constant of 100 kcal/mol Å^2. Optimizations were performed only for the active site region. Residues further than 10 Å

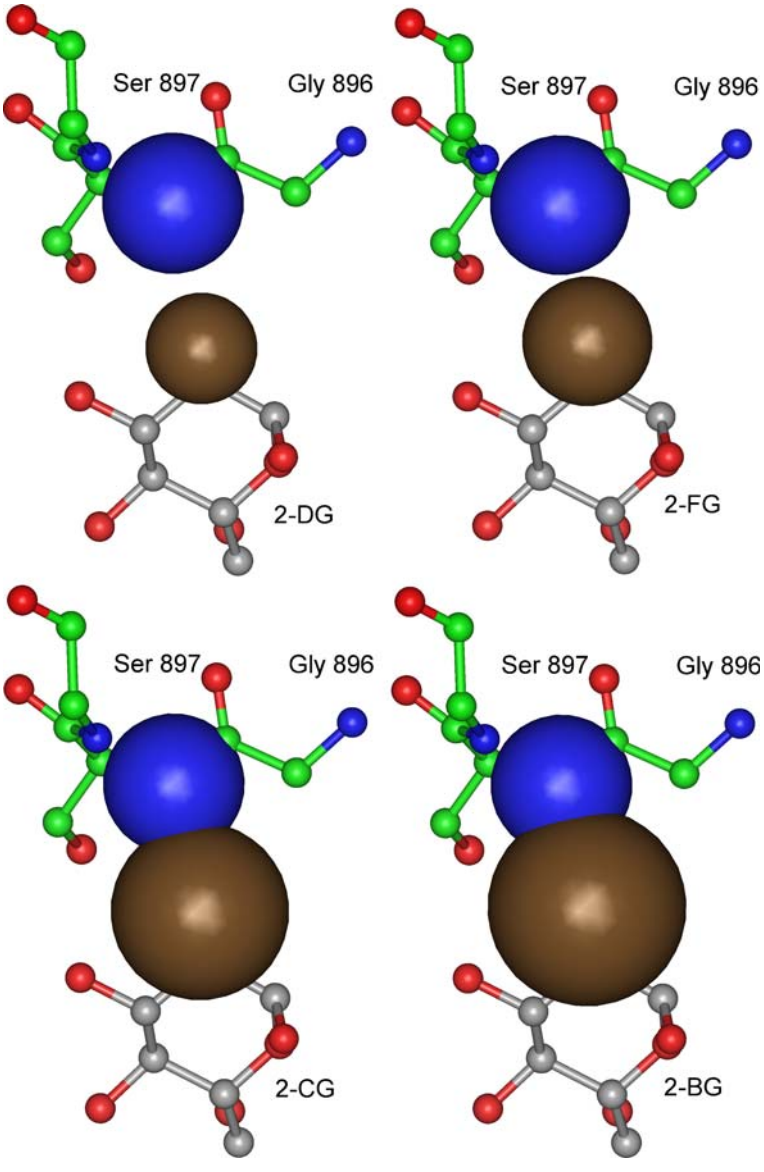

Fig. 2 A schematic "cartoon-type" representation of (a) 2-DG (2-DG-6P), (b) 2-FG (2-FG-6P), (c) 2-CG (2-CG-6P), and (d) 2-BG (2-BG-6P) in the G-6P binding site of hexokinase I, depicting differences in the relative size of the halogens and increasing steric hindrance for chlorine and bromine. Both hexokinase I (*green carbons*) and ligands (*gray carbons*) are shown as balls and sticks. Selected atoms, N (*blue*) of Ser897 in hexokinase I and H, F, Cl, Br (*brown*) of the glucose analogs, are shown as CPK. Since, the phosphate group of G-6P does not influence the steric effect, it is not displayed. Please note that G-6P analogs with the undisplayed phosphate group is identical to glucose analogs

from the active center were fixed to avoid uncontrolled global conformational changes of the protein.

Calculation of binding energies

In this study, a simple QSAR-like approach along with a flexible docking strategy using MM methods were applied [8, 34]. In the case where a ligand binds in a single well-defined conformation to a tight binding pocket of the protein molecule, it is expected that the binding free energy of the complex ΔA_{BIND} correlates well with the MM energies obtained from a constrained energy minimization of the complex and the following relationship holds:

$$\Delta A_{\mathrm{BIND}} \sim E_{\mathrm{min}}^{\mathrm{complex}} - E_{\mathrm{min}}^{\mathrm{protein}} - E_{\mathrm{min}}^{\mathrm{ligand}}.$$

The minimized energy of the complex ($E_{\mathrm{min}}^{\mathrm{complex}}$) is obtained as the final MM energy after optimization of this system. The protein and ligand structures are extracted separately from the minimized complex, and their respective energies, ($E_{\mathrm{min}}^{\mathrm{protein}}$) and ($E_{\mathrm{min}}^{\mathrm{ligand}}$) were computed without any further minimization. The term corresponding to the protein energy was averaged for all structures obtained with various ligands.

Results

Molecular modeling

Comparison of human hexokinase sequences suggests that their active site regions should be nearly identical. Moreover, because the four human hexokinase types (I–IV) have high sequence similarity (52–77% of sequence identity), modeling carried out for hexokinase I is assumed to be representative for all of them. During preparation of this article, an experimental structure of the human glucokinase (hexokinase IV), which is the most dissimilar in sequence compared with the other human hexokinases, was determined [13]. This structure superimposes on the hexokinase I C-terminal domain with an average deviation of 0.9 Å for 417 Cα atom pairs, which results in perfect superposition of the glucose (GLC) binding sites and the bound glucose molecules as well. Slight differences observed in the G-6P binding sites are most likely due to the lack of a G-6P in the glucokinase structure; however, a similar conformation of this region is expected after ligand binding. This confirms that the modeling results obtained for hexokinase I can be generalized for the remaining human hexokinases.

Figure 2 illustrates the effects of substituting halogens at the C-2 position of glucose and demonstrates that the fit into G-6P binding-pocket of hexokinase is best mimicked by fluorine due to its size. Moreover, the increasing size of the halogens (i.e. F < Cl < Br) leads to steric hindrance, which destabilizes binding of the respective phosphorylated glucose analogs. When considering the potential ability of the halogen analogs to bind to hexokinase due to the number of hydrogen bonds they can form, it is found to be less than that of glucose but greater than that of 2-DG. Thus, on the basis of molecular modeling considerations, 2-FG should more favorably interact with hexokinase than 2-DG. This qualitative finding correlates well with the binding energies (Table 1) computed with the procedure described above.

The two possible sites on hexokinase where the glucose and G-6P derivatives could bind are at the original GLC binding site and the original G-6P binding site. We applied molecular modeling methods to estimate binding affinities of phosphorylated and non-phosphorylated glucose analogs to both binding sites. Due to the simplifications inherent in our modeling approach, the absolute values of the binding energies presented in Table 1 cannot be considered exact, because slight changes in model parameters result in relatively high-energy variations. However, the relative order as well as the differences in the binding energies between the first three molecules (D-glucose, 2-DG, 2-FG) and the remaining ones was conserved (data not shown). As expected, the phosphorylated molecules showed higher affinities to the G-6P binding site than did their non-phosphorylated counterparts, and the non-phosphorylated molecules showed higher affinities to the GLC binding site than to the G-6P one. Our modeling results also suggested that D-glucose, 2-DG, and 2-FG can be phosphorylated by hexokinases with very similar rates, whereas for the remaining 2-halo-analogs the binding affinities to the GLC site are much lower and rapidly decrease with the increased size of the halogen atom.

Lactate (a measure of glycolysis) decreases as a function of decreasing halogen size

On the basis of the molecular modeling results presented above, we hypothesized that after forming their respective 6-phosphate intermediates, 2-FG > 2-CG > 2-BG in inhibiting phosphoglucose isomerase, the next step in the glycolytic pathway. When lactate is used as an endpoint of this pathway, it is clear from the data presented in Fig. 3 that the potency (ID_{50}s) to inhibit glycolysis indeed follows this prediction when ρ^{o} cells are treated for 24 h. Moreover, this same relationship applies when ρ^{o} cells are treated for 24 h with the same dose of each analog (Fig. 3b).

Cytotoxicity in hypoxic cells increases as halogen size decreases

When glycolysis is blocked by an inhibitor, such as 2-DG in the genetic model of "hypoxia," ρ^{o} cells, and or in the environmental model of hypoxia (wild type cells in 0.5% oxygen) that depend solely on glycolysis for

Table 1 Theoretical binding energies (kcal/mol) of D-glucose, glucose-6-phosphate and their analogs

Phosphorylation state	Non-phosphorylated at C-6		Phosphorylated at C-6
Molecule	Binding energy at the GLC site	Binding energy at the G-6P site	Binding energy at the G-6P site
D-Glucose	−8.6	−4.6	−19.2
2-Deoxy-D-glucose (2-DG)	−7.8	−2.5	−14.8
2-Fluoro-D-glucose (2-FG)	−7.8	−4.8	−18.3
2-Chloro-D-glucose (2-CG)	2.9	5.2	−8.6
2-Bromo-D-glucose (2-BG)	8.1	8.7	−4.8

survival, the cells die [21]. In contrast, the aerobically growing wild type parental cells 143B, with functional mitochondria, survive glycolytic inhibition by using carbon sources other than glucose (fats and proteins) to generate ATP via oxidative phosphorylation [22, 25, 30]. Moreover, since the intermediates of the glycolytic pathway are important as anabolic precursors for DNA, RNA, glycoproteins, and glycolipids [31], blockage of this pathway leads to growth inhibitory effects in aerobic as well as anaerobic cells [21]. Using these differences in "hypoxic" versus aerobic cell responses to drugs allows for the determination of whether glucose analogs halogenated at C-2, target the glycolytic pathway and thereby either inhibit cell growth and/or kill cells.

When the potency of these analogs to induce cytotoxicity was assayed by both trypan blue exclusion and flow cytometry, "hypoxic" cells were found to be much more affected than were normoxic cells by 2-FG (Figs. 4a,5a,b). This difference in toxicity between hypoxic and normoxic cells was lower for the chloro analog 2-CG and was further reduced for the bromo analog 2-BG (Fig. 4a). If the cytotoxic potency is considered for each of the analogs, it is clear that 2-FG > 2-CG > 2-BG in killing "hypoxic" cells, which also corresponds to their abilities to inhibit growth in both cell types (Fig. 4b). These results are consistent with molecular modeling and the lactic acid results, indicating that the less favorable binding with hexokinase resulting from the increasing the size of the halogen leads to reduced potencies to inhibit glycolysis.

2-FG is more potent than 2-DG in blocking glycolysis and killing hypoxic cells

When 2-DG was compared with 2-FG at similar doses in both cytotoxic assays, we found that 2-FG was more potent in killing "hypoxic" cells (Figs. 4a,5a,b). These results agree with the data shown in Fig. 3, demonstrating that 2-FG is more potent than 2-DG in lowering lactic acid levels and consequently blocking glycolysis in "hypoxic" cells. Interestingly, at high doses of 2-DG there was a slight but statistically significant induction of cell death in the wt cells (Figs. 4a,5b) that did not occur with 2-FG, even though 2-FG decreased lactic acid levels in these cells more efficiently than did 2-DG (data not shown).

Discussion

In previous studies it was found that 2-DG competes with D-glucose for transport into cells as well as for hexokinase, the first step of glycolysis [38]. We reported that 2-DG inhibits the growth of 143B parental cells under normoxic conditions and at equivalent doses,

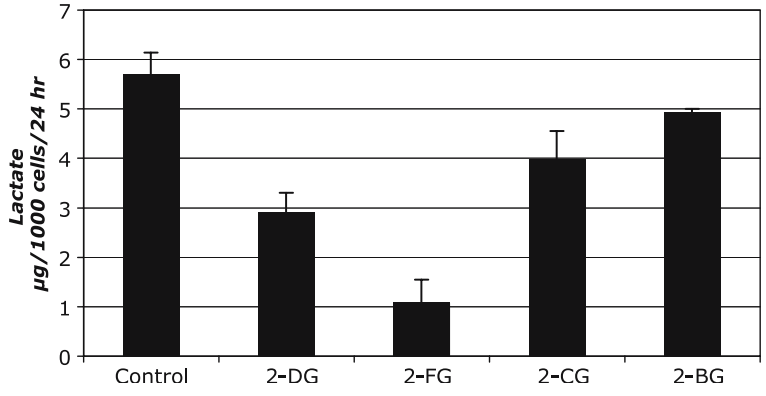

Fig. 3 Comparative potencies of 2-DG and halogen-substituted 2-carbon glucose analogs to inhibit lactic acid production. **a** Lactic acid levels, as expressed in µg/10^3 cells/24 h, were measured in ρ^o cells treated at the same dose (3 mM) for 24 h, with 2-DG, 2-FG, 2-CG, or 2-BG. The results show that 2-FG > 2-DG > 2-CG > 2-BG in inhibiting lactic acid at this dose. **b** This agrees with the lactic acid ID_{50}s measured for these compounds

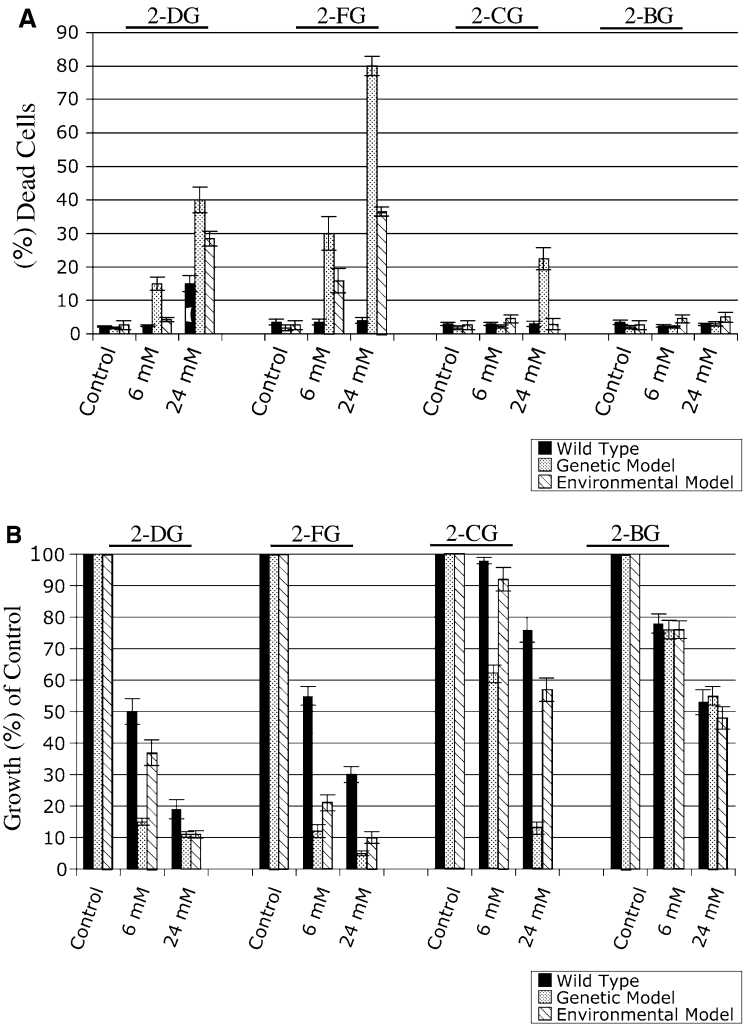

Fig. 4 Cytotoxic and growth inhibitory potencies of 2-DG, 2-FG, 2-CG, and 2-BG in 143B and ρ^o cells. **a** Cytotoxicity as measured by trypan blue exclusion assay of aerobic (143B, *white columns*) versus genetic (ρ^o, *black columns*) and environmental (*gray columns*) "hypoxic" cell models treated with 6 or 24 mM of 2-DG, 2-FG, 2-CG, or 2-BG for 72 h. **b** Growth inhibitory assays of aerobic (143B, *white columns*) versus genetic (ρ^o, *black columns*) and environmental (*gray columns*) "hypoxic" cell models treated with 6 or 24 mM of 2-DG, 2-FG, 2-CG, or 2-BG for 72 h

"hypoxic" cells are growth inhibited to a greater degree and also undergo cell death [18, 21]. Our data indicate that as the halogen substituent in the glucose analogs studied here gets larger, the selectivity between "hypoxic" and normoxic (wt.) cells decreases (Figs. 4a,b). Moreover, it is clear that as the halogen size decreases, the potency of these sugar analogs to induce growth inhibition, cytotoxicity, and cell cycle perturbations in hypoxic cells increases (Fig. 5). These results can best be interpreted by assuming that as the size of the halogen substituent increases, the ability of the glucose derivatives to fit into the hexokinase pocket diminishes, which results in the reduction of the respective 6-O-phosphorylated intermediates required to block the glycolytic pathway. This interpretation is consistent with our findings that the binding energies follow the order 2-FG > 2-CG > 2-BG, for both the phosphorylated and non-phosphorylated forms of these analogs at the two binding sites, i.e. GLC and G-6P of hexokinase (Table 1). Furthermore, the ability of these analogs to block the glycolytic pathway as measured by lactic acid levels also follows the same order (Fig. 3). Our results in intact human cells are in agreement with studies performed on isolated yeast hexokinase in which 2-FG was found to be a better substrate than 2-CG [4]. Moreover, since it has been shown that hexokinase can be inhibited by G-6P but not by 2-DG-6P [6] and that inhibition by G-6P occurs at both active (GLC) and allosteric (G-6P) sites, our data (Table 1) suggests that 2-FG-6P may be similar to G-6P in allosteric inhibition of hexokinase [19]. Thus, in addition to hexokinase producing greater amounts of 2-FG-6P than 2-DG-6P as predicted by molecular modeling, which will lead to greater inhibition of phosphoglucose isomerase, a contributing mechanism to explain 2-FG having greater potency than 2-DG by inhibiting glycolysis and killing hypoxic cells, may be via allosteric inhibition of hexokinase. Although our experiments cannot rule out the possibility that differences in drug transport due to halogen size may also be a contributing factor to our results, nevertheless the molecular modeling and lactic acid results are consistent with the data, which illustrate that 2-FG > 2-CG > 2-BG in preferentially inhibiting cell growth and killing hypoxic versus aerobic cells.

Although in both "hypoxic" models it is clear that cells are more sensitive to 2-FG than to the other

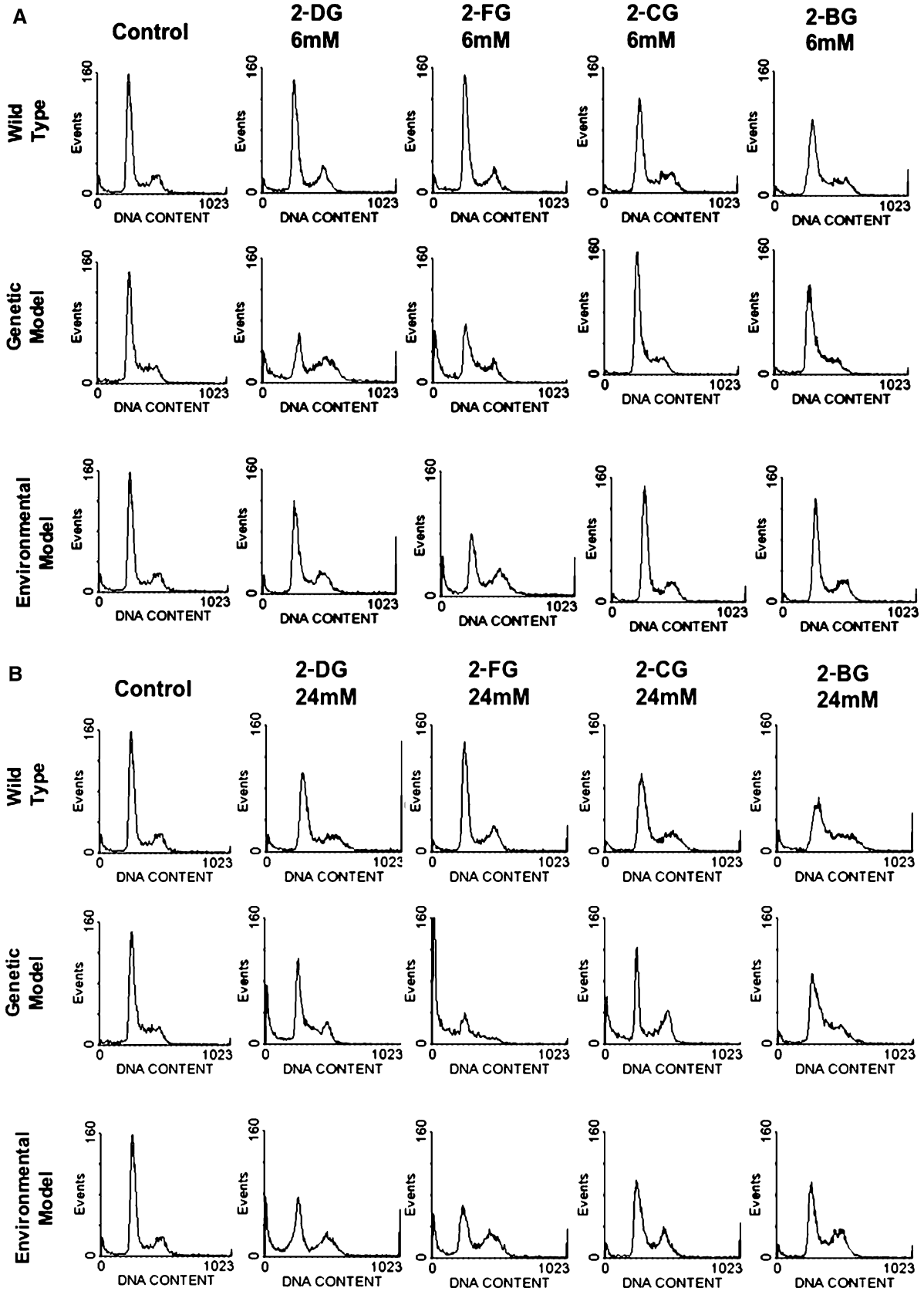

Fig. 5 Flow cytometric DNA content analysis of aerobic (143B) versus genetic (ρ^o) and environmental "hypoxic" cell models treated with 6 mM (**a**) and 24 mM (**b**) of 2-DG, 2-FG, 2-CG, or 2-BG for 72 h

halogenated analogs, the genetic model shows greater sensitivity than the environmental one. A major difference between the two hypoxic models is the expression of HIF [36] in the environmental model, which could explain its decreased sensitivity to glycolytic inhibitors since the greater amount of glycolytic enzymes that results from HIF would require increased amounts of glycolytic inhibitors. Another possible mechanism that may be occurring is the up regulation of antiapoptotic proteins when cells are placed under low oxygen tension [9], which would render these cells less sensitive to glycolytic inhibition. Both mechanisms are under investigation in our laboratories.

When 2-FG was compared directly with 2-DG using flow cytometry, we found that a concentration of 24 mM, 2-FG produced severe effects in the genetic model (ρ^o cells), almost completely eliminating them from the G1, S, and G2/M phases and less severe but nevertheless significant toxicity in the environmental hypoxic cell model. In comparison, treatment with 2-DG caused less cell death and a significantly higher proportion of cells accumulated and survived in both models (Fig. 5b). At low doses the difference in the effects between 2-FG and 2-DG on the cell cycle seem even more pronounced in both hypoxic models (Fig. 5a), which correlates with the greater potency of 2-FG compared to 2-DG to inhibit lactic acid production. The direct cytotoxicity assays showed somewhat less of a difference in the number of cells killed by 2-FG (80% in the genetic model; 35% in the environmental model) compared with 2-DG (45% in the genetic model; 27% in the environmental model) at high doses (24 mM) than when assayed by flow cytometry. This discrepancy between trypan exclusion assays and flow measurements most likely derives from the heightened sensitivity of flow cytometry, in which 10,000 cells are counted as compared to that of trypan blue exclusion assay using a hemocytometer where significantly less cells are analyzed (< 20). Moreover, since the flow cytometry assay used here measured DNA content, dead cells that had disintegrated could be detected by measuring broken DNA, whereas only intact dying or dead cells could be detected with the trypan blue exclusion assay. Again molecular modeling and the lactic acid results are consistent with the data indicating that 2-FG > 2-DG in preferentially inhibiting cell growth and killing "hypoxic" versus aerobic cells in both models.

Another distinguishing difference between 2-FG and 2-DG was that 2-FG at 24 mM produced no detectable cytotoxicity in aerobic cells, whereas at the same dose 2-DG did cause death in these cells. Taking into account the fact that 2-FG is more potent than 2-DG in inhibiting lactic acid production and in killing hypoxic cells, mechanisms other than blockage of glycolysis likely account for the toxicity of 2-DG in the normoxic cells. Moreover, because aerobically respiring cells with competent mitochondria are able to use fats and proteins as energy sources when glycolysis is blocked, they should be able to survive this type of treatment, which reinforces the idea that at a high dose, 2-DG but not 2-FG kills aerobic cells by means other than inhibition of glycolysis. In this regard, it has been shown that 2-DG interferes with the process of glycosylation in viral coat formation differently than does 2-FG [35]. Thus, it is possible that at high doses (24 mM) of 2-DG, wt. cells may be dying due to interference with glycosylation of certain glycoproteins that 2-FG does not affect. This is an area of interest that our laboratory is currently investigating.

2-FG has shown the remarkable ability to preferentially accumulate in tumor versus normal tissues as demonstrated using positron emitting ^{18}F-labeled 2-FG and PET scan. Our findings demonstrate that 2-FG (the non-radioactive form) is more potent than 2-DG in blocking glycolysis and consequently killing hypoxic cells, as well as being less toxic to aerobic cells. Therefore, since 2-DG is currently in phase I clinical trials to determine its efficacy for enhancing standard chemotherapy by killing hypoxic tumor cells, our results suggest that 2-FG may be even more effective clinically in targeting this slow-growing cell population found in most, if not all, solid tumors.

Acknowledgment Supported by NIH grant R01 CA037109 16, SPORE grant in Pancreatic Cancer P20 CA101936 a grant from The Morton and Angela Topfer Pancreatic Cancer Research Fund, and BST funds of Warsaw University.

References

1. Adamson J, Foster AB (1969) 2-Chloro-2-deoxy-D-glucose and 2,2-dichloro-2-deoxy-D-arabino-hexose. Carb Res 10:517–523
2. Albert M, Dax K, Ortner J (1998) A novel direct route to 2-deoxy-2-fluoro-aldoses and their corresponding derivatives. Tetrahedron 54:4839–4848
3. Aleshin AE, Kirby C, Liu XF et al (2000) Crystal structures of mutant monomeric hexokinase I reveal multiple ADP binding sites and conformational changes relevant to allosteric regulation. J Mol Biol 296:1001–1015
4. Bessell EM, Foster AB, Westwood JH (1972) The use of deoxyfluoro-D-glucopyranoses and related compounds in a study of yeast hexokinase specificity. Biochem J 128:199–204
5. Brown J (1962) Effects of 2-deoxyglucose on carbohydrate metabolism: review of the literature and studies in the rat. Metabolism 11:1098
6. Crane RK, Sols A (1954) The non-competitive inhibition of brain hexokinase by glucose-6-phosphate and related compounds. J Biol Chem 210:597–606
7. Di Raddo P, Diksic M (1986) Fluorination of 3,4,6-tri-O-acetyl-1,5-anhydro-2-deoxy-D-arabino-hex-1-enitol in water. Carb Res 153:141–145
8. Gordon RK, Ginalski K, Rudnicki WR et al (2003) Anti-HIV-1 activity of 3-deaza-adenosine analogs—Inhibition of S-adenosylhomocysteine hydrolase and nucleotide congeners. Eur J Biochem 270:3507–3517
9. Greijer AE, van der Wall E (2004) The role of hypoxia inducible factor 1 (HIF-1) in hypoxia induced apoptosis. J Clin Pathol 57:1009–1014
10. Hoekstra C, Paglianiti I, Hoekstra O (2000) Monitoring response to therapy in cancer using [18F]-2-fluoro-2-deoxy-D-glucose and positron emission tomography: an overview of different analytical methods. Eur J Nucl Med 27:731–743
11. Hwang M-J, Stockfisch TP, Hagler AT (1994) Derivation of class II force fields. II. Derivation and characterization of a class II force field, CFF93, for the alkyl functional group and alkane molecules. J Am Chem Soc 116:2515–2525

12. Kalir T, Wang BY, Goldfischer M, Haber RS et al (2002) Immunohistochemical staining of GLUT1 in benign, borderline, and malignant ovarian epithelia. Cancer 94:1078–1082
13. Kamata K, Mitsuya M, Nishimura T et al (2004) Structural basis for allosteric regulation of the monomeric allosteric enzyme human glucokinase. Structure 12:429–438
14. King MP, Attardi G (1989) Human cells lacking mtDNA: repopulation with exogenous mitochondria by complementation. Science 246:500–503
15. Krishan A, Paika K, Frei E (1975) Cytofluorometric studies on the action of podophyllotoxin and epipodophyllotoxins (VM-26, VP-16-213) on the cell cycle traverse of human lymphoblasts. J Cell Biol 66:52
16. Lampidis TJ, Priebe W (2003) Cancer chemotherapy with 2-deoxy-D-glucose. US Patent 6,670,330,B1, 30 Dec 2003
17. Larson S, Grunbaum Z, Rasey J (1980) Positron imaging feasibility studies: selective tumor concentration of ^{3}H-thymidine, ^{3}H-uridine, and ^{14}C-2-deoxyglucose. Radiology 134:771–773
18. Liu H, Hu YP, Savaraj N, Priebe W, Lampidis TJ (2001) Hypersensitization of tumor cells to glycolytic inhibitors. Biochemistry 40:5542–5547
19. Liu X, Kim CS, Kurbanov FT et al (1999) Dual mechanisms for glucose 6-phosphate inhibition of human brain hexokinase. J Biol Chem 274:31155–1159
20. Liu H, Savaraj N, Priebe W, Lampidis TJ (2002) Hypoxia increases tumor cell sensitivity to glycolytic inhibitors a strategy for solid tumor therapy (Model C). Biochem Pharmacol 64:1746–1751
21. Maher JC, Krishan A, Lampidis TJ (2004) Greater cell cycle inhibition and cytotoxicity induced by 2-deoxy-D-glucose in tumor cells treated under hypoxic versus aerobic conditions. Cancer Chemother Pharmacol 53:116–122
22. McKeehan WL (1982) Glycolysis, glutaminolysis, and cell proliferation. Cell Biol Int Rep 6:635–650
23. Maple JR, Hwang M-J, Stockfisch TP et al (1994) Derivation of class II force fields. I. Methodology and quantum force field for the alkyl functional group and alkane molecules. J Comput Chem 15:162–182
24. Maschek G, Savaraj N, Priebe W (2004) 2-Deoxy-D-Glucose increases the efficacy of adriamycin and paclitaxel in human osteosarcoma and non-small cell lung cancers in vivo. Cancer Res 64:31–34
25. Mazurek S, Boschek CB, Eigenbrodt E (1997) The role of phosphometabolites in cell proliferation, energy metabolism, and tumor therapy. J Bioenerg Biomembr 29:315–327
26. Nirenberg MW, Hogg JF (1958) Inhibition of anaerobic glycolysis in Ehrlich ascites tumor cells by 2-deoxy-D-glucose. Cancer Res 18:518
27. Noguchi Y, Marat D, Saito A et al (1999) Expression of facilitative glucose transporters in gastric tumors. Hepatogastroenterology 46:2683–2689
28. Ortner J, Albert M, Weber H, Dax K (1999) Studies on the reaction of D-glucal and its derivatives with 1-chloromethyl-4-fluoro-1,4-diazoniabicyclo[2.2.2]octane salts. J Carb Chem 18:297–316
29. Rappe AK, Goddard WAI (1991) Charge equilibration for molecular dynamics simulations. J Phys Chem 95:3358–3363
30. Reitzer LJ, Wice BM, Kennell D (1979) Evidence that glutamine, not sugar, is the major energy source for cultured HeLa cells. J Biol Chem 254:2669–2676
31. Reitzer LJ, Wice BM, Kennell D (1980) The pentose cycle: control and essential function in HeLa cell nucleic acid synthesis. J Biol Chem 255:5616–5626
32. Rohren EM, Turkington TG, Coleman RE (2004) Clinical applications of PET in oncology. Radiology 231:305–332
33. Rudlowski C, Becker AJ, Schroder W et al (2003) GLUT1 messenger RNA and protein induction relates to the malignant transformation of cervical cancer. Am J Clin Pathol 120:691–698
34. Rudnicki WR, Kurzepa M, Szczepanik T et al (2000) A simple model for predicting the free energy of binding between anthracycline antibiotics and DNA. Acta Biochim Pol 47:1–9
35. Schmidt MF, Biely P, Kratky Z, Schwarz RT (1978) Metabolism of 2-deoxy-2-fluoro-D-[3H]glucose and 2-deoxy-2-fluoro-D-[3H]mannose in yeast and chick-embryo cells. Eur J Biochem 87:55–68
36. Semenza GL (2003) Targeting HIF-1 for cancer therapy. Nat Rev Cancer 10:721–732
37. Sharma V, Luker GD, Piwnica-Worms D (2002) Molecular imaging of gene expression and protein function in vivo with PET and SPECT. J Magn Reson Imaging 16: 336–351
38. Wachsberger PR, Gressen EL, Bhala A et al (2002) Variability in glucose transporter-1 levels and hexokinase activity in human melanoma. Melanoma Res 12:35–43
39. Teichman M, Descotes G, Lafont D (1993) Bromination of 1,5-anhydrohex-1-enitols (glycals) using quarternary ammonium tribromides as bromine donors: synthesis of α-1,2-trans-2-bromo-2-deoxyglycopyranosyl bromides and fluorides. Synthesis 889–894
40. Wahl R, Hutchins G, Buchsbaum D (1991) 18F-2-deoxy-2-fluoro-D-glucose (FDG) uptake into human tumor xenografts: feasibility studies for cancer imaging with PET. Cancer 67:1544–1550
41. Wick AN, Drury DR, Nakada HI, Wolfe JB (1957) Localization of the primary metabolic block produced by 2-deoxyglucose. J Biol Chem 224:963
42. Zingone A, Seidel J, Aloj L et al (2002) Monitoring the correction of glycogen storage disease type 1a in a mouse model using [(18) F] FDG and a dedicated animal scanner. Life Sci 71:1293–1301